Journal Pre-proof

Synthesis and biological evaluation of [^{18}F](2S,4S)4-(3-fluoropropyl) arginine as a tumor imaging agent

Renbo Wu, Song Liu, Yajing Liu, Yuli Sun, Xuebo Cheng, Yong Huang, Zequn Yang, Zehui Wu

PII: S0223-5234(19)30882-7

DOI: https://doi.org/10.1016/j.ejmech.2019.111730

Reference: EJMECH 111730

To appear in: *European Journal of Medicinal Chemistry*

Received Date: 9 August 2019

Revised Date: 21 September 2019

Accepted Date: 21 September 2019

Please cite this article as: R. Wu, S. Liu, Y. Liu, Y. Sun, X. Cheng, Y. Huang, Z. Yang, Z. Wu, Synthesis and biological evaluation of [^{18}F](2S,4S)4-(3-fluoropropyl) arginine as a tumor imaging agent, *European Journal of Medicinal Chemistry* (2019), doi: https://doi.org/10.1016/j.ejmech.2019.111730.

This is a PDF file of an article that has undergone enhancements after acceptance, such as the addition of a cover page and metadata, and formatting for readability, but it is not yet the definitive version of record. This version will undergo additional copyediting, typesetting and review before it is published in its final form, but we are providing this version to give early visibility of the article. Please note that, during the production process, errors may be discovered which could affect the content, and all legal disclaimers that apply to the journal pertain.

© 2019 Published by Elsevier Masson SAS.

Graphical Abstract

To create your abstract, type over the instructions in the template box below.

Synthesis and Biological Evaluation of [^{18}F](2S,4S)4-(3-fluoropropyl)-Arginine as a Tumor Imaging Agent

Renbo Wu,[a] Song Liu,[a] Yajing Liu,[b] Yuli Sun,[a] Yong Huang,[a] Zequn Yang,[a] and Zehui Wu[a]*

Leave this area blank for abstract info.

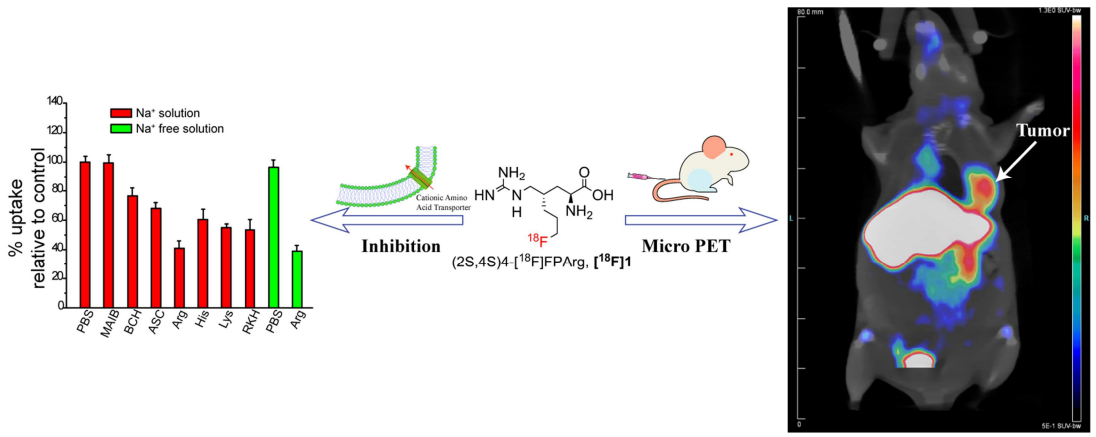

Journal

Journal Pre-proof

ELSEVIER

journal homepage: www.elsevier.com

Synthesis and Biological Evaluation of [^{18}F](2S,4S)4-(3-fluoropropyl) Arginine as a Tumor Imaging Agent

Renbo Wu,[a] *Song Liu,*[a] *Yajing Liu,*[b] *Yuli Sun,*[a] *Xuebo Cheng,*[a] *Yong Huang,*[a] *Zequn Yang*[a] *and Zehui Wu*[a*]

[a] *Beijing Institute of Brain Disorders, Capital Medical University, Beijing, 100069, China;*
[b] *School of Pharmaceutical Science, Capital Medical University, Beijing 100069, China.*

ARTICLE INFO

Article history:
Received
Revised
Accepted
Available online

Keywords:
Arginine
Breast Cancer
Imaging agent
Cationic Amino Acid Transporter,
Positron Emission Tomography

ABSTRACT

Designing novel ^{18}F-labeled amino acid derivatives for targeted amino acid transporters is an attractive strategy for the development of therapeutic and diagnostic agents for cancer therapy. In this work, we have developed a novel 3-fluoropropyl analog of arginine, namely, (2S,4S)4-[^{18}F]FPArg, **[^{18}F]1**, to be used as a probe for studying arginine metabolism. Optically pure and labeled with ^{18}F and ^{19}F, (2S,4S)4-(3-fluoropropyl)arginine was synthesized and isolated in high radiochemical purity (>95%). In vitro uptake assays in human MCF-7 cells revealed that **[^{18}F]1** enters cells mainly via sodium-independent cationic amino acid transporters and was inhibited >62% by arginine. **[^{18}F]1** showed a high cellular uptake of 7.3 ± 0.24% and 6.07 ± 0.3% uptake/100 mg protein after incubation in MCF-7 and MDA-MB-231 cells for 120 min, respectively. In vivo biodistribution studies demonstrated that **[^{18}F]1** provided high tumor uptake and high tumor to muscle ratios (5:1 at the 30 and 60 min time points). In vivo PET imaging studies demonstrated tumor-specific uptake in nude mice bearing MCF-7 breast tumors with an excellent tumor-to-muscle ratio. These results suggest that **[^{18}F]1** is a promising tracer for clinical breast cancer imaging and may be used to diagnose and monitor diseases that are associated with arginine metabolism.

1. Introduction

Radiolabeled amino acids are structurally and functionally diverse tumor imaging agents suitable for positron emission tomography (PET) and single photon emission computed tomography (SPECT), which have been used extensively for oncologic imaging in both preclinical and human clinical studies.[1-4] Imaging agents determined by their amino acid transporters can potentially provide uniquely and clinically biological tumor information.[1] Traditionally, the amino acid transporter family has been functionally characterized as a transport system, such as system L, system A, system N, system ASC, system xCT and cationic amino acid transporter (CAT), many of which contain multiple family members.[5-10] The research and identification of new radiolabeled amino acids with novel features has focused on targeting system L and ASC because they are upregulated in various human cancers.[3, 10-14] Many imaging agents targeting system L (e.g., [^{11}C] MET,[15, 16] [^{18}F] FET,[17-19] [^{18}F] FDOPA,[20, 21] [^{123}I] IMT,[22]) and system ASC ([^{18}F] FMA,[23] [^{11}C] Gln,[24] [^{18}F] (2S, 4R)4-FGln,[25, 26] [^{18}F] (2S,4R)4-FPGln,[27] anti-3-[^{18}F] FACBC[28]) have been reported in the past few decades (Figure 1). Imaging agent targeting system A (e.g., S-[^{18}F] FAMP and S-[^{18}F] MeFAMP[29]) and system xCT (e.g., [^{18}F] (2S,4R)4F-Glu[30] and [^{18}F] (2S,4S) FSPG[30]) have also been gaining interest (Figure 1). Among these, targeting system L imaging agents are widely used in the diagnosis of clinical gliomas because they can cross the blood-brain barrier.[16, 31, 32] [^{18}F](2S,4R)4-FGln has been demonstrated to be useful in detecting breast tumors in women.[33] ^{18}F(2S, 4S)FSPG has a high cancer detection rate in patients with hepatocellular carcinoma.[34] Anti-3-[^{18}F] FACBC (Axumin) has been approved by the FDA for routine clinical applications of prostate cancer. Recently, amino acid imaging agent development has explored cationic amino acid transport systems for oncologic imaging, such as the cationic tyrosine analog O-2((2-[^{18}F]fluoroethyl)methyl-amino)ethyltyrosine ([^{18}F]FEMAET) selective for target system ATB$^{0,+}$.[5] The 1H-[1,2,3] triazole substituted amino acid ((S)-[^{18}F]AFETP) is mediated by a combination of cationic amino acid transport and system L transport.[35] [^{18}F] AFETP is expected to be used for the early detection of the tumor response to arginine depletion due to ADI-PEG20 treatment.[36] Though studies have shown that cationic amino acid transport is increasingly recognized as important targets for oncology imaging and therapy,[3, 36-38] imaging agents of natural cationic amino acid derivatives, such as L-arginine and L-lysine, have not been reported yet. Therefore, designing and synthesizing natural cationic amino acid derivative imaging agents are particularly urgent.

Corresponding authors.
E-mail addresses: wzhhuey2012@ccmu.edu.cn

Journal Pre-proof

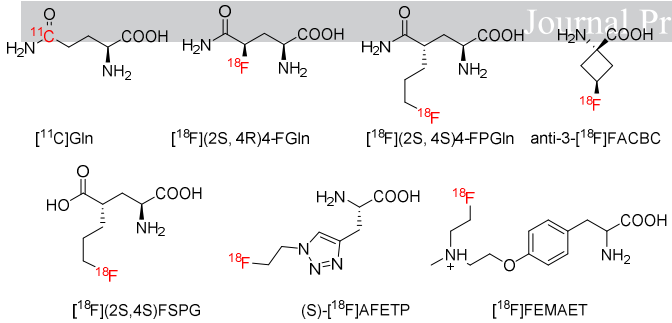

Fig. 1. Chemical structures of [^{11}C]Gln, [^{18}F](2S,4R)4-FGln, [^{18}F](2S,4S)4-FPGln, anti-3-[^{18}F]FACBC, [^{18}F](2S,4S)FSPG, (S)-[^{18}F]AFETP and [^{18}F]FEMAET

Arginine is a cationic amino acid which can be synthesized from citrulline in two steps by the urea cycle enzymes argininosuccinate synthetase and argininosuccinate lyase[37, 39]. Arginine is closely related to the tumor suppression, carcinogenesis and the biological behavior of tumors through various biological metabolic pathways.[40, 41] Some normal cells are able to synthesize arginine from citrulline by argininosuccinate synthetases (ASS). However, the expression of ASS is lacking in some tumor cells such as melanoma and hepatocellular carcinoma, which renders the arginine auxotrophy of the tumor. The requirement of exogenous arginine for cellular growth, proliferation and survival in ASS lacking tumor provides an important strategy for the development of therapeutic and diagnostic agents for cancer.[3, 42] Therefore, L-arginine and its analogs could serve as biomarkers for oncologic imaging in terms of detection, prognosis and response to therapeutic monitoring of arginine metabolism-related tumors. Herein, we report the first efficient organic and radiosynthetic routes to obtain the L-arginine derivative (2S,4S)4-FPArg, **1**. This novel tracer was evaluated both in vitro cell uptake assays and in vivo biodistribution studies and PET/CT imaging with nude mice transplanted with human MCF-7 tumor.

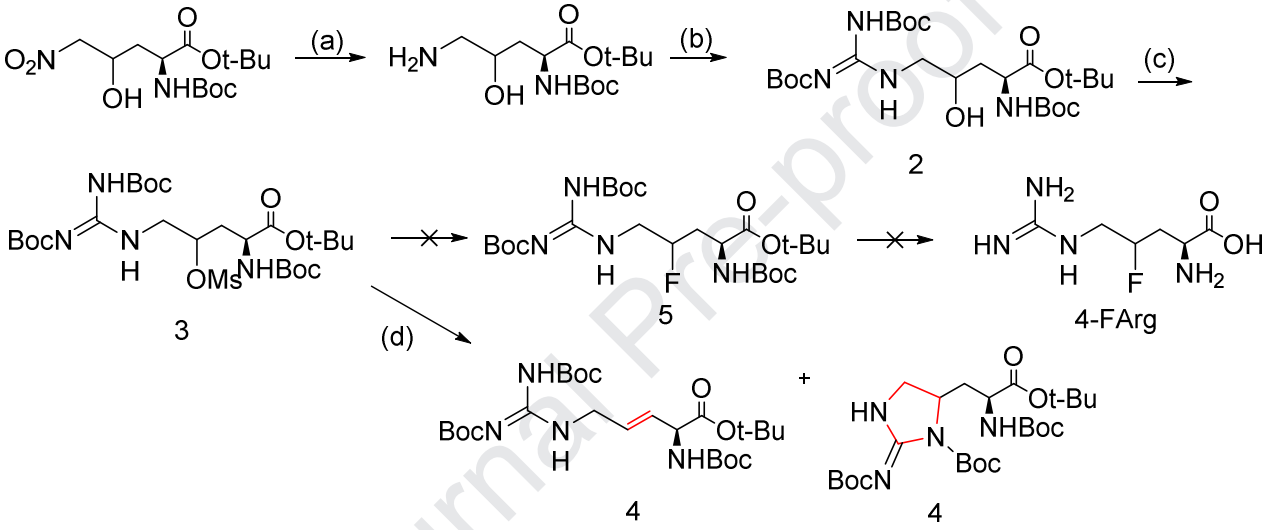

Reagents and conditions: (a) Pd/C, methanol, rt, 3h; (b) N,N′-Di-Boc-1H-pyrazole -1-carboxamidine, N,N-Diisopropylethylamine, ACN, 50 °C, 3h; (c) Methanesulfonyl chloride, Et_3N, DCM, rt, 4h; (d) TASF, $Et_3N{\cdot}(HF)_3$, CH_2Cl_2/THF, 55 °C, overnight.

Scheme 1. An attempt to synthesis of **4-FArg**

2. Results and discussion

2.1. Synthesis

Our strategy was to modify the carbon at position 4 of arginine based on the analysis of the arginine structure and the experience of synthesizing glutamine derivatives.[25, 27] **4-FArg** was first considered to be synthesized because the structure of arginine was minimally altered (Scheme 1). The synthesis of compound **2** was obtained by the guanidinylation of the amino group with N, N'-Di-Boc-1H-pyrazole-1-carboxamidine according to the reported procedure.[43] Surprisingly, the tosylation reaction of **2** did not work, probably because the steric hindrance from the carbon at position 4 in arginine was too large. The activating group was replaced by a less sterically hindered methanesulfonyl chloride, and **3** was obtained in low yield (32%). In the reaction solution, **3** easily converted to **4** (checked by LC-MS). Unfortunately, the fluorination reactions cannot provide any of the desired product **5** regardless of whether the fluorinating reagent is tetrabutylammonium fluoride, potassium fluoride or tris(dimethylamino) sulfonium difluorotrimethylsilicate (TASF). We reasoned that the NH groups of guanidine of arginine attacked the activated ester at position 4 of arginine to form a stable five-membered ring. Therefore, at least one of the NH groups of guanidine of arginine must be protected, but the protected arginine cannot introduce an activated ester at carbon 4 due to the large steric hindrance, and the corresponding **4-FArg** cannot be obtained. **4-FArg** may be obtained by introducing a fluorine atom into the starting material and then performing a multistep reaction. However, radiosynthesis is complicated to operate and has low yields, which is not conducive to clinical application.

To obtain a radioactive arginine derivative with simple labeling conditions, we tried to introduce a fluoropropane at the carbon at position 4 of the arginine (Scheme 2, (2S,4S)4-(3-fluoropropyl)arginine, (2S,4S)4-FPArg, **1**), which will make the fluorine SN2 substitution reaction on the primary carbon easier and will not racemize during the labeling reaction. According to the experience from the synthesis of **4-FArg**, at least one NH at carbon position 2 or 5 of the precursor of **1** must be protected, and a six-membered ring can be formed easily by the NH at carbon position 5, which reacts with the sulfonyl ester; therefore, the NH at carbon position 5 was selected for protection. Following our design (Scheme 2), **7**

Journal Pre-proof

was obtained by our reported synthetic method.[27] Compound **7** was mixed with an anhydride, followed by reduction with sodium borohydride to give **8** in a total yield of 85%. Notably, guanidinylation of **8** is a critical step in the whole scheme. A Mitsunobu reaction was carried out by using **8**, N, N'-Di-Boc-1H-pyrazole-1-carboxamidine, triphenylphosphine and diethyl azodicarboxylate to give **9** in 89% yield (Scheme 2). This step enabled the introduction of the NH (carbon at position 5 of arginine protected) with a tert-butoxycarbonyl (Boc) protecting group. The next step involved coupling of a suitable amino protecting group that could be easily removed after radiolabeling. 4-Methoxybenzyl was chosen as the amino protecting group because it is easily removed in the presence of TFA. Substituting 4-methoxybenzylamine for the activated ester (pyrazole) of **9** gave **10** in 75% yield. Removal of the OH protecting group in **10** by pyridinium p-toluenesulfonate gave **11** in 84% yield. Tosylation of **11** gave tosylate **12** (the precursor for fluorination) in 86% yield. The O-tosylated **12** was treated with TASF and $Et_3N(HF)_3$ to give the desired compound **13** in 55% yield. Optimization of the fluorination reaction conditions using TASF and $Et_3N(HF)_3$ as the reagents that were reported previously for the preparation of 4-fluoroglutamine.[27] Deprotection using TFA at room temperature produced the final products, (2S,4S)4-FPArg, **1** in 93% yield. To better distinguish the peaks of the isomers produced during the labeling reaction and to investigate the ability of tumors to take up D and L arginine, we synthesized the corresponding isomer of **1**, (2R,4R)4-FPArg, **25**, using the same synthesis method as **1** (Scheme 2 and S1).

.

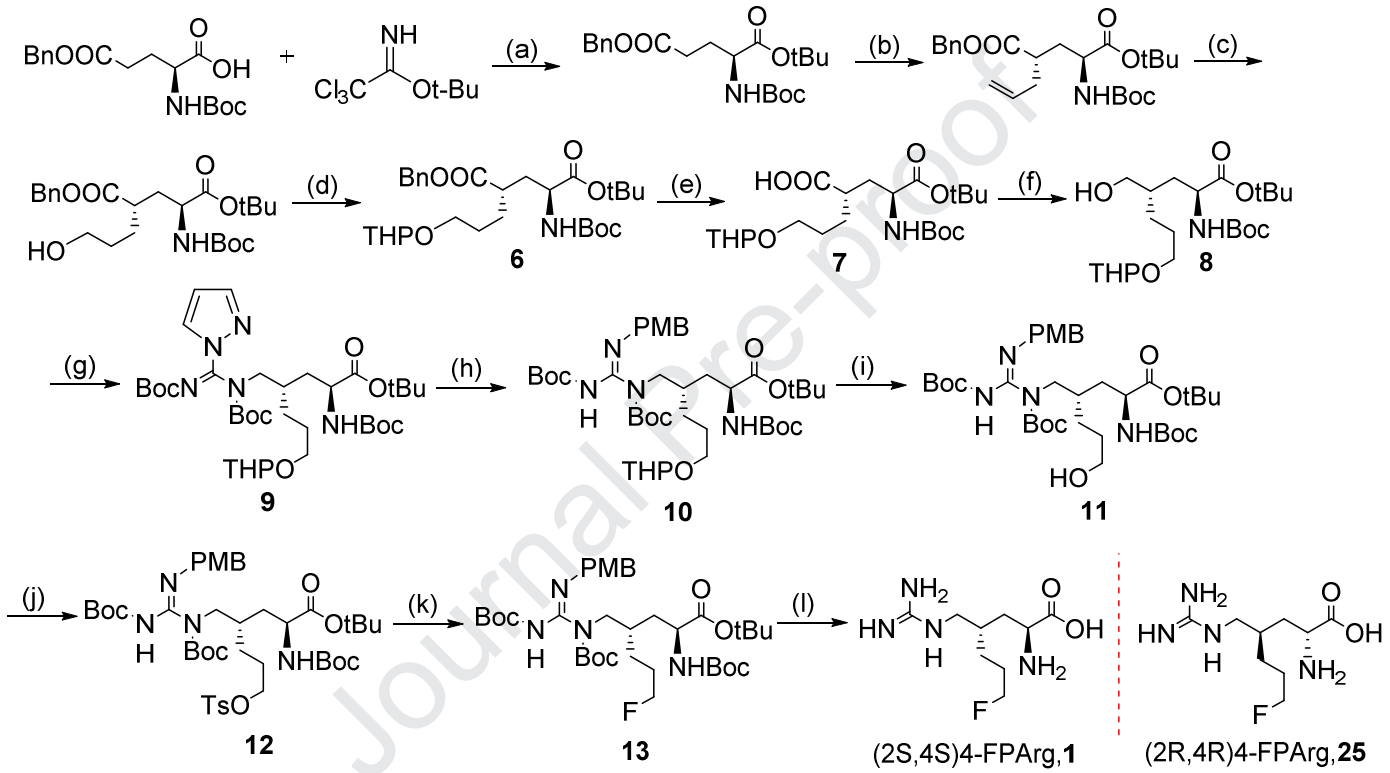

Reagents and conditions: (a) tert-butyl 2,2,2-trichloroacetimidate (TBTA), $BF_3{\cdot}Et_2O$, DCM, cyclohexane, rt, overnight; (b) LiHMDS, Allyl bromide, THF, -78 °C, 4 h; (c) 9-BBN, H_2O_2, NaOH, 0 °C - rt, 48 h; (d) DHP, PPTS, DCM, rt, 3 h; (e) Pd/C, H_2, EtOH, rt, 2 h; (f) Ethyl chloroformate, $NaBH_4$, THF, H_2O, 0 °C - rt, 4 h; (g) N,N′-Di-Boc-1H-pyrazole-1-carboxamidine, triphenyl phosphine, diethyl azodicarboxylate, THF, 0 °C - rt, overnight; (h) 4-Methoxybenzylamine, *N*,*N*-Diisopropylethylamine, ACN, 3h; (i) PPTS, ethanol, 2h; (j) p-toluenesulfonyl chloride, Et_3N, DCM, rt, overnight; (k) TASF, $Et_3N{\cdot}(HF)_3$, CH_2Cl_2/THF, 55 °C, overnight; (l) TFA, rt, overnight.

Scheme 2. Synthesis of (2S,4S)4-FPArg, **1** and structure of (2S,4S)4-FPArg, **25**

2.2. Radiolabeling and Stability

The radiosynthesis was conducted in two steps (Scheme 3). Initially, the radiosynthesis was conducted in two steps following the (2S,4R)4-[^{18}F]FPGln labeling method,[27] but the radiolabeling failed despite trying to increase the temperature or change the solvent (entries 1-3). According to Kim's method,[44, 45] the tert-amyl alcohol solvent system may have some beneficial effects on the mechanism of nucleophilic substitution; therefore, tert-amyl alcohol was selected as the reaction solvent for the labeling reaction. Kryptofix 222 was first chosen as the phase transfer catalyst for the labeling reaction; surprisingly, the yield was still very low, and the product was racemic (Figure S4a and entry 4). The precursor, **12**, was converted into **26** or **27** as determined by the LC-MS analysis of the first step reaction solution (Figures 2a, S1 and Table 1, entries 1-4), which indicates that the elimination reaction was faster than the nucleophilic substitution reaction during the reaction. This problem may be solved by protecting the NH at the carbon at position 2. To our delight, 18-crown-6 replaced Kryptofix 222 as the phase transfer catalyst, and the labeling yield was greatly improved when the reaction solution was acetonitrile/tert-amyl alcohol (1/9) (Table 1, entry 5). A large amount of the labeled precursor was unreacted as the fluorinated reactant was detected by LC-MS, therefore, the labeling conditions were further optimized by increasing the amount of the phase transfer catalyst. When the amount of the phase transfer catalyst was doubled, the labeling yield increased from 3.52% to 5.93% (Table 1, entry 6). Further increasing the temperature of the reaction, the labeling yield continued to improve (Table 1, entry 7). In summary, the labeling reaction was carried out in two steps. The first step, nucleophilic [^{18}F] fluoride substitution, was successfully

performed in tert-amyl alcohol/acetonitrile (9/1) at 100 °C to afford the intermediate **[^{18}F]13** from pure precursor **12**. Using solid phase extraction with a C18 cartridge, the **[^{18}F]13** was retained while the unreacted [^{18}F] fluoride was removed. Then, the **[^{18}F]13** was eluted from the cartridge with ethanol. The radiochemical purity of **[^{18}F]13** was determined by radiometric thin-layer chromatography (ethyl acetate/petroleum ether = 2/3, Rf = 0.6) and analytical HPLC (Figure S2). In the second step, deprotection was achieved with TFA, followed by removal of the reaction solution. A solution containing 10% ethanol in physiological saline was added and passed through a 0.22 μm nylon filter to provide the final product (2S,4S)4-[^{18}F]FPArg, **[^{18}F]1**(log P = -0.72). Radiochemical purity was determined by chiral analytic HPLC (Figure 2b and S4). Notably, first step was purified by a solid phase column, and occasionally two radioactive peaks were observed (ethyl acetate/petroleum ether = 2/3, Rf = 0.4 and 0.6, Figure S3). We speculate the other radioactive peak may due to the removal of one or more Boc groups from intermediate **[^{18}F]13**. This is because only the target compound **[^{18}F]1** was obtained when the mixture of the first reaction was hydrolyzed by TFA. **[^{18}F]1** displayed high stability in PBS buffer (10 mM, pH = 7.4) at room temperature and plasm at 37 °C for 2 h, as confirmed by radio-HPLC (Figure 3a). The radiolabeling of **[^{18}F]25** was consistent with the radiolabeling conditions of **[^{18}F]1** (Scheme S2).

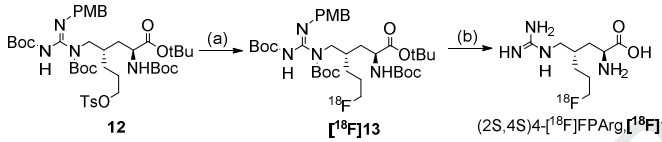

Reagents and conditions: (a) 1 mL of 18-crown-6/$KHCO_3$ (320 mg of 18-crown-6 in 18.6 mL of ACN/58 mg of $KHCO_3$ in 3.4 mL of water), 100 °C, 15 min, tert-amyl alcohol and acetonitrile (9/1); (b) TFA, anisole, 60 °C, 5 min.

Scheme 3. Radiosynthesis of (2S,4S)4-[^{18}F]FPArg, **[^{18}F]1**

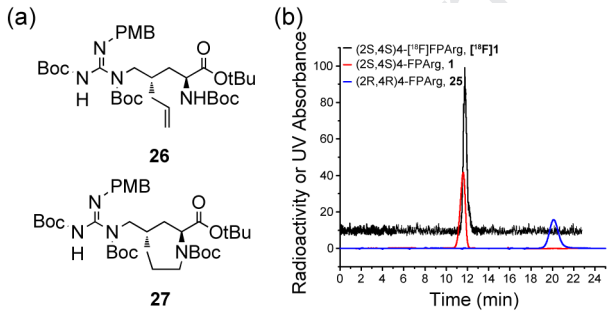

Fig. 2. (a) Structures of two byproducts in labeling reaction; (b) HPLC profiles of (2S,4S)4-FPArg, **1**, (2R,4R)4-FPArg, **25** and (2S,4S)4-[^{18}F]FPArg, **[^{18}F]1,** using HPLC system (Column: Chirex 3126 (D)-penicillamine 250 × 4.6 mm, 4.6 μm). Mobile phase (isocratic): Methanol/1 mM $CuSO_4$= 5/95.

Table 1. The optimal conditions for (2S,4S)4-[^{18}F]FPArg, **[^{18}F]1**

Entry	Reaction conditions	Yield[f]	Epimerization
1	(1) 18-crown-6, $KHCO_3$, 80 °C, 15 min, ACN [a b]	0.57 ± 0.15%	NO
2	(1) 18-crown-6, $KHCO_3$, 100 °C, 15 min, ACN [a b]	1.04 ± 0.21%	NO
3	(1) 18-crown-6, $KHCO_3$, 100 °C, 15 min, DMSO [a b]	1.08 ±0.19%	NO
4	(1) K_{222}, K_2CO_3, 100 °C, 15 min, tert-amyl alcohol [c b]	1.42 ± 0.23%	Yes
5	(1) 18-crown-6(160 mg), $KHCO_3$(28 mg), 90 °C, 15 min, tert-amyl alcohol and acetonitrile (9/1) [d b]	3.52 ± 0.56%	NO
6	(1) 18-crown-6(320 mg), $KHCO_3$(58 mg), 90 °C, 15 min, tert-amyl alcohol and acetonitrile (9/1) [d b]	5.93 ± 1.01%	NO
7	(1) 18-crown-6(320 mg), $KHCO_3$(58 mg), 100 °C, 15 min, tert-amyl alcohol and acetonitrile (9/1) [d b]	6.95 ± 1.51%	NO

(a) 1 mL 160 mg 18-Crown-6 in 18.6 mL acetonitrile/29 mg $KHCO_3$ in 3.4 mL water; (b) TFA/anisole (495/5), 60 °C, 5 min; (c) 1 mL 220 mg K_{222} in 18.6 mL acetonitrile/40 mg K_2CO_3 in 3.4 mL water; (d) 1 mL 18-Crown-6 in 18.6 mL acetonitrile/ $KHCO_3$ in 3.4 mL water. (f) yield uncorrected, n = 3.

2.3. Cell Uptake Assays and Inhibition Studies

MCF-7 (ER+) and MAD-MB-231 (ER-), the two typical types of breast cancer are chosen for uptake capacity study. One reason for the selection is based on estrogen receptor (ER) expression level, which determines the following treatment strategy optimization. The other is the membrane presentation of transporters, which is crucial for our interested biological function. Previous study has showed that argininosuccinate synthetase 1 (ASS1) expression level is highly related to the subcellular localization of CAT-1[36] and the mRNA level of ASS1 is high in MCF-7 (log2(RPKM) = 7.99) and low in MAD-MB-231 (log2(RPKM) =1.89) [CCLE, https://portals.broadinstitute.org/ccle]. However, the cation transporters present in both cell types are primarily CAT-1 subtypes.[46] Both cells can uptake and accumulate **[^{18}F]1** from 5 min to 120 min, which suggests **[^{18}F]1** can be used as a tracer for the diagnosis of ER+ and ER- breast cancers (Figure 3b). However, the corresponding isomer **[^{18}F]25** showed a lower uptake in both cells, which is consistent with the high uptake of the L-type natural amino acid reported in the literature.[25] Additionally, whether for **[^{18}F]1** or **[^{18}F]25**, the uptake by MCF-7 cells is higher than that by MDA-MB-231 cells at the late stage. The result is accordance with the membrane presentation level of CAT-1. **[^{18}F]25** was not further subjected to biological evaluation due to the low uptake of **[^{18}F]25** by the tumor cells. The in vitro cell uptake of **[^{18}F]1**, **[^{18}F]FDG** and [^{18}F](2S, 4R)4-FGln in MCF-7 cell was further compared. As Figure 3c exhibited, in vitro cell uptake of **[^{18}F]1** showed lower uptake than [^{18}F](2S, 4R)4-FGln and **[^{18}F]FDG** in MCF-7 cell culture for 5 min to 120 min.

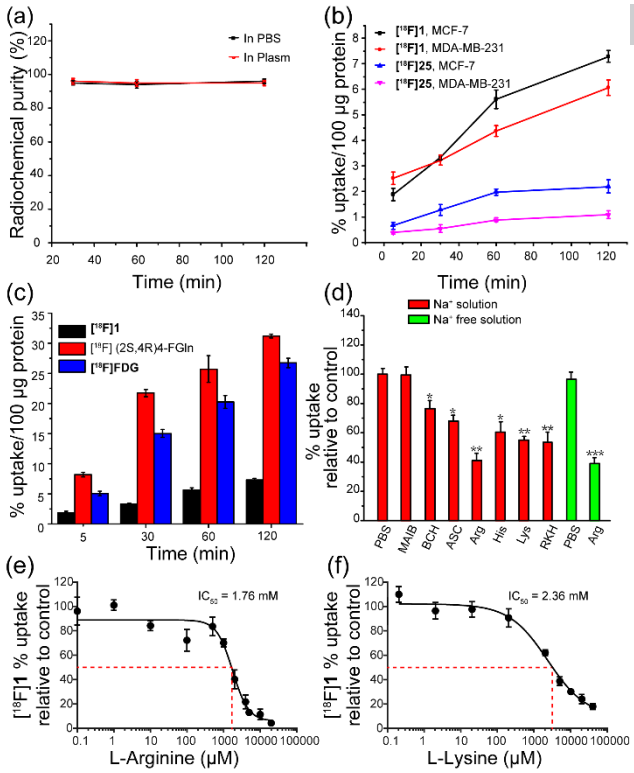

Fig. 3. (a) The stability in PBS and Plasm of (2S,4S)4-[^{18}F]FPArg, **[^{18}F]1** (n = 3) (b) In vitro cell uptakes of **[^{18}F]1** in MCF-7 and MDA-MB-231 cell lines, (n = 5) (c) In vitro cell uptakes of **[^{18}F]FDG**, [^{18}F](2S, 4R)4-FGln and **[^{18}F]1** in MCF-7, (n = 5). At the same time point, the cell uptake of **[^{18}F] 1** was compared with **[^{18}F]FDG** (significantly different at 4 time points are less than 0.001), [^{18}F](2S, 4R)4-FGln (significantly different at 4 time points are less than 0.001), respectively. (d) In vitro cell uptake inhibition studies of **[^{18}F]1** conducted in MCF-7 cells, incubation 30 min. Na solution= PBS buffer, Na free solution = K or choline replacement Na PBS buffer, MeAIB = 10 mM N-methyl a aminoisobutyric acid (system A inhibitor), BCH = 10 mM aminobicyclo(2,2,1)-heptane-2-carboxylic acid (system L inhibitor), Arg = 10 mM arginine, His = 10 mM histidine, Lys = 10 mM lysine, ASC = a mixture of L-Ala, L-Ser, L-Cys (3.3 mM of each amino acid), RKH = L-Arg, L-Lys, L-His mixture (3.3 mM of each amino acid). The sodium PBS control condition was compared to the PBS BCH*, ASC*, His*, Arg**, Lys** and RKH** (*, $p < 0.05$ and **, $p < 0.01$) condition using two-tailed t tests. The choline PBS control condition was compared to the choline PBS Arg (***, $p < 0.01$) condition using two-tailed t tests. IC_{50} assay: inhibition of **[^{18}F]1** uptake by increasing different concentrations of L-Arg (e) or L-Lys (f), incubation 120 min. Each data point is n = 5.

The mechanisms of transport of **[^{18}F]1** were assessed through in vitro uptake assays with MCF-7 cells in the absence and presence of amino acid transport inhibitors. A variety of inhibitor conditions were used to determine which amino acid transport system or systems were responsible for the cell uptake of **[^{18}F]1**. As shown in Figure 3d, there was no uptake inhibition of **[^{18}F]1** in the presence of MeAIB, indicating that **[^{18}F]1** did not use system A to enter MCF-7 cells. In contrast, the uptake of **[^{18}F]1** under Na BCH and Na ASC conditions was 76 ± 5.5% ($p < 0.05$) and 67 ± 4.1% ($p < 0.05$) relative to the control, respectively (Figure 3d). These results indicate a component of systems L and ASC transport **[^{18}F]1**. Because **[^{18}F]1** is a derivative of L-arginine, the basic side chain amino acids L-arginine, L-histidine and L-lysine individually and together (RKH) were selected as competitive inhibitors for inhibition assays. In the presence of 10 mM L-lysine, approximately 48% of the **[^{18}F]1** uptake by MCF-7 cells was blocked relative to the sodium control ($p < 0.01$). The uptake of **[^{18}F]1** in the Na histidine and Na RKH conditions was 60 ± 7.2% ($p < 0.05$) and 53 ± 6.8% ($p < 0.01$) relative to the control, respectively (Figure 3d). The uptake of **[^{18}F]1** was partially blocked by arginine with 40 ± 5.2% uptake relative to the sodium control ($p < 0.01$). As expected, the arginine conditions inhibited 62% of the uptake relative to the sodium-free control ($p < 0.01$), indicating that the cell uptake of **[^{18}F]1** was mainly mediated by sodium-independent cationic amino acid transport (Figure 3d). From the above experimental results, it can be seen that arginine has a stronger inhibitory effect on **[^{18}F]1** than lysine, but the usual transport proteins of the CAT family have similar Km values to arginine and lysine. To investigate the differential inhibition of arginine compared with lysine, the half-maximal inhibitory concentrations (IC_{50}, mM) of arginine and lysine were measured (Figure 3e-f). The results indicate that arginine (IC_{50} = 1.76 mM) exhibits a higher affinity than lysine (IC_{50} = 2.36 mM) for the CAT family of transport proteins. It has been reported that cation transporter proteins in MCF-7 cells mainly include CAT-1, CAT-2A and CAT-2B, and CAT-1 plays an important role in the cellular uptake of arginine.[46] The CAT-1 protein shows a higher affinity for amino acids, while CAT-2A and CAT-2B show a lower affinity.[47, 48] The CAT proteins seem to have a higher affinity for cationic amino acids with a long carbon backbone.[49] Combined with the above reports and the results of this experiment, we can conclude that the order of affinity for CAT proteins is **[^{18}F]1** > arginine > lysine, the inhibition rate of arginine for **[^{18}F]1** should be higher than lysine, and **[^{18}F]1** may be a high-affinity CAT-1 transporter substrate. Taken together, the cationic amino acid transport substrate L-arginine was the most effective inhibitor of **[^{18}F]1** uptake. These findings suggest that a significant proportion of the in vitro uptake of **[^{18}F]1** is mediated by cationic amino acid transporters, although other amino acid transporters that recognize neutral amino acids, including systems L and ASC also contribute. More extensive amino acid transport assays will be needed to determine which of these transport systems mediate the uptake of **[^{18}F]1** by MCF-7 cells.

2.4. Biodistribution Studies

The results of the biodistribution studies with nude mice with subcutaneous MCF-7 tumors at 5, 30, 60 and 120 min postinjection (p.i.) are shown in Table 2 and are expressed as the percent of the total injected dose per gram of tissue (% ID/g). The tumor uptake of **[^{18}F]1** was rapid with 1.6 ± 0.21 % ID/g at 5 min and remained relatively constant over the course of the study to 1.78 ± 0.25 % ID/g at 30 min and 1.68 ± 0.13 % ID/g at 60 min (Table 2). A slow wash out was observed for the tumor uptake and retention in the MCF-7 tumor to 1.14 ± 0.07 % ID/g at 120 min p.i. At 30 min, the tumor-to-background (tumor-to-muscle and tumor-to-blood) ratios of **[^{18}F]1** were 5.34 ± 0.83 and 4.61 ± 0.81, respectively. At each time point, the brain uptake of **[^{18}F]1** was relatively low. As shown in Table S1, maximal blood, liver and kidney uptake of **[^{18}F]1** in BALB/c mice were rapid with 3.48 ± 0.79 % ID/g, 22.88 ± 3.68 % ID/g and 24.98 ± 5.33 % ID/g respectively, 5 min after the injection with progressive washout at 30, 60 and 120 min, which is consistent with the biodistribution of nude mice bearing MCF-7 tumors (Table 2). The highest levels of uptake for **[^{18}F]1** in nude mice bearing MCF-7 tumors were observed in the kidneys and livers at the 5, 30 and 60 min time points, but pancreatic uptake was relatively moderate and constant at the same time points (Table 2), which is different from the common pattern seen with radiolabeled amino acids. The uptake of **[^{18}F]1** was prominent in the kidney, liver and urinary bladder, indicating that the radiotracer was mainly excreted by the kidney and liver. In other organs including the muscle, spleen, heart and stomach, the uptake was low to moderate (Table 2). The bone uptake of **[^{18}F]1** was relatively constant, indicating that no in vivo defluorination occurred over the time course of the study (Table 2). **[^{18}F]1** showed moderate uptake in the large and small intestines uptake in nude mice bearing MCF-7 tumors with a relatively slow washout rate (Table

Pre-proof
Journal Pre-proof

Journal Pre-proof

2), which was consistent with the reported better uptake of arginine by the intestine.[50]

Further differences in the biodistribution of **[^{18}F]FDG**, [^{18}F](2S,4R)4-FGln and **[^{18}F]1** in nude mice bearing MCF-7 tumors were compared. Unlike **[^{18}F]1**, at 60 min and 120 min p.i., the heart uptake was the highest in all organs in the **[^{18}F]FDG** biodistribution study (Table S2), and the pancreas uptake was the highest for the [^{18}F](2S, 4R)4-FGln study.[33] **[^{18}F]1** (Table 2) exhibited a faster clearance compared to **[^{18}F]FDG** (Table S2) and [^{18}F](2S, 4R)4-FGln **(**T/B, 6.37 ± 0.45 and 1.52 ± 0.16**)** at 60 min and 120 min p.i..[33] The tumor to muscle ratio observed with **[^{18}F]1** (Table 2) and [^{18}F](2S, 4R)4-FGln **(**T/M, 3.91 ± 0.42) were much higher than with **[^{18}F]FDG** (Table S2, $p < 0.01$) at 60 min p.i. due to the much higher uptake of **[^{18}F]FDG** in muscle,[33] indicating that **[^{18}F]1** and [^{18}F](2S, 4R)4-FGln would be useful for imaging breast cancer. At 120 min p.i., the T/M of **[^{18}F]1** was still significantly higher than **[^{18}F]FDG** (Table S2, $p < 0.01$) and [^{18}F](2S, 4R)4-FGln (1.52 ± 0.16, $p < 0.05$),[33] indicating that **[^{18}F]1** has a wider range of optimal imaging times.

Table 2. In Vivo Biodistribution of **[^{18}F]1** in nude mice bearing MCF-7

organ	5 min	30 min	60 min	120 min
blood	2.29 ± 0.54	0.37 ± 0.08	0.22 ± 0.05	0.11 ± 0.01
tumor*	1.60 ± 0.21	1.78 ± 0.25	1.68 ± 0.13	1.14 ± 0.07
brain	0.14 ± 0.04	0.07 ± 0.01	0.09 ± 0.01	0.06 ± 0.01
heart	1.13 ± 0.25	0.34 ± 0.04	0.34 ± 0.05	0.25 ± 0.03
liver	10.73 ± 1.32	6.36 ± 0.60	4.34 ± 0.51	1.67 ± 0.28
spleen	0.79 ± 0.13	0.63 ± 0.10	0.53 ± 0.06	0.34 ± 0.02
lung	2.25 ± 0.29	0.92 ± 0.09	0.84 ± 0.12	0.57 ± 0.10
kidney	16.2 ± 2.13	6.01 ± 0.63	2.94 ± 0.38	1.21 ± 0.10
muscle	0.53 ± 0.13	0.4 ± 0.16	0.39 ± 0.19	0.39 ± 0.06
bone	1.28 ± 0.24	1.17 ± 0.19	2.01 ± 0.18	1.78 ± 0.22
skin	1.88 ± 0.06	0.71 ± 0.05	0.77 ± 0.12	0.77 ± 0.29
pancreas	3.01 ± 0.54	3.91 ± 0.46	3.26 ± 0.36	1.79 ± 0.22
large intestine	1.83 ± 0.25	1.58 ± 0.38	1.47 ± 0.07	1.31 ± 0.06
small intestine	2.95 ± 0.37	2.81 ± 0.33	2.93 ± 0.53	2.33 ± 0.48
bladder	6.37 ± 1.29	1.52 ± 0.31	1.65 ± 0.46	1.29 ± 0.21
stomach	1.60 ± 0.69	0.89 ± 0.14	0.93 ± 0.11	0.64 ± 0.11
tumor/blood(T/B)	0.72 ± 0.15	4.61 ± 0.81	7.68 ± 1.41	10.05 ± 0.91
tumor/muscle(T/M)	3.19 ± 0.78	5.34 ± 0.83	4.31 ± 1.12	2.89 ± 0.81

[a] 1.29 MBq of **[^{18}F]1** was administrated via tail vein injection without anesthesia. The animals were euthanized at 5, 30, 60, 120 min (n = 5) after injection. The data are expressed as mean % ID/g with standard deviation. There was significant difference in tumor and muscle uptake values after 5 min ($p < 0.01$), 30 min ($p < 0.01$), 60 min ($p < 0.001$), and 120 min ($p < 0.001$) of injection.

2.5. Small Animal PET/CT Imaging in nude Mice Bearing MCF-7 Tumors and blocking study

To further investigate tumor uptake, tumor imaging of **[^{18}F]1** was studied using a dynamic small animal PET study of a nude mice with MCF-7 tumors. As demonstrated by Figure 4a, the MCF-7 tumors could be visualized with **[^{18}F]1**. The relatively low normal brain uptake of **[^{18}F]1** may be due to the exclusion of these tracers by the BBB. High liver, kidney and bladder uptake were also observed. The relatively low levels of activity in the bone indicated that no substantial in vivo defluorination occurred during the 180 min time course of the study. To assess the in vivo kinetics, a region of interest analysis was performed to generate a time-activity curve (Figure 4b). The kinetic curves confirmed that the tracers exhibited higher uptake in the tumor compared to the muscle (background) regions. In addition, the tumor uptake still

Journal Pre-proof

increased at 3 h, indicating that the tumor has high uptake and high retention of **[^{18}F]1** (Figure 4b). The SUV of tumor uptake continued to increase, which was different than the biodistribution result. The reason for this difference is not clear but may be due to the effects of anesthesia during the small animal PET studies. Within 3 h, the liver still exhibited high uptake, which is consistent with the literature reports that the liver has a higher uptake of arginine.[51] These results clearly indicate that **[^{18}F]1** is suitable as a breast cancer imaging tracer.

To further confirm that **[^{18}F]1** is specific for the CAT protein, microPET imaging with **[^{18}F]1** uptake blocked by arginine in the same mice was performed. As shown in Figure 4c, the SUV of tumor uptake was reduced from 3.6 ± 0.24 to 2.9 ± 0.15 (relative to no arginine inhibition, $p < 0.05$) when the amount of pretreated arginine was 0.5 mg. As the amount of arginine was further increased to 2 mg, the SUV of tumor uptake was further reduced to 2.4 ± 0.21 (relative to no arginine inhibition, $p < 0.05$, Figure 4c), suggesting potent in vivo competitive binding of arginine with **[^{18}F]1** for the CAT protein.

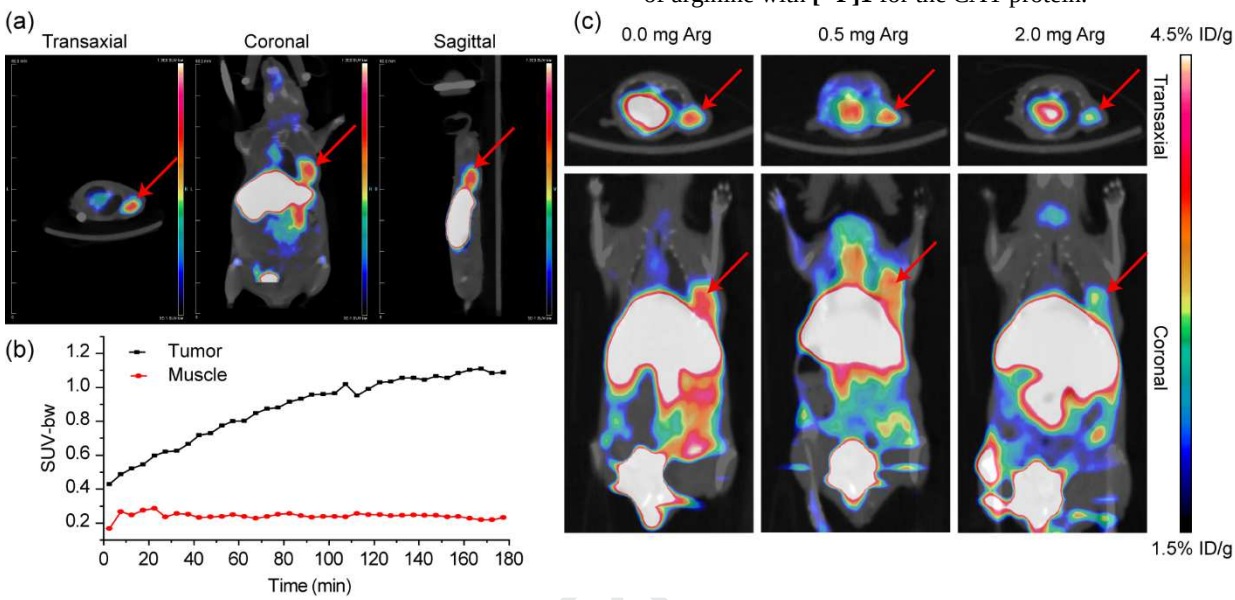

Fig. 4. Representative PET images of MCF-7 tumor-bearing nude mice after intravenous injection of **[^{18}F]1** into nude mice (n = 3). The images of the views (a) are from a summed 3 h scan. (b) Time-activity curves of **[^{18}F]1** uptake in tumor and muscle. (c) Small-animal PET images of MCF-7 tumor-bearing nude mice at 45 - 65 min p.i. of **[^{18}F]1** with (left) 0 mg, 0.5 mg (middle) and 2 mg (right) injection of arginine. The red arrows represent the location of tumors.

The targeted CAT tracers [^{18}F]AFETP and [^{18}F]FEMAET have been reported for many years, but neither have been clinically used. [^{18}F]FEMAET is most likely to selectively targets $ATB^{0,+}$, which can reflect the $ATB^{0,+}$ activity in vivo through PET imaging.[5, 52] However, [^{18}F]FEMAET still needs to be further developed because it is not an optically pure compound, and the effect of the proportion of its racemate on the imaging has not been considered.[5, 52] [^{18}F]AFETP is mainly mediated by LAT and CAT, its synthesis is simple and the labeling yield is high. It is expected to be used for the diagnosis of high-grade gliomas and to monitor the response of tumors to arginine depletion treatment. Compared with [^{18}F]AFETP and [^{18}F]FEMAET, the radiolabeling conditions of **[^{18}F]1** are simple and easy to handle their labeling success rate is high, and the yield is stable. However, the labeling yield of **[^{18}F]1** is low, and it is still necessary to further optimize the reaction conditions and the structure of the radiolabeling precursor. The unique advantage of **[^{18}F]1** is that it can reflect the physiological function of arginine to a great extent because it possesses all of the functional groups of arginine and its uptake may be mediated by the same transporter as arginine.

Preliminary in vitro cell uptake experiments showed that MCF-7 cells uptake of **[^{18}F]FDG** and [^{18}F](2S, 4R)4-FGln were much higher than **[^{18}F]1**, which may be because glucose and glutamine are the two main nutrients used by cancer cells for proliferation and survival. Comparing the biodistribution data, it can be seen that the tumor uptake of **[^{18}F]FDG**, [^{18}F](2S, 4R)4-FGln and **[^{18}F]1** were high at 60 min p.i., but due to the higher background of **[^{18}F]FDG**, the T/M ratio is lower and the image contrast is not high enough. **[^{18}F]1** has a longer washout time in tumor than [^{18}F](2S, 4R)4-FGln (more than 1 hour), and the T/M ratio is higher and the optimal imaging time is wider. Comparing the previous reported PET imaging data of [^{18}F](2S, 4R)4-FGln,[33] the T/M value of **[^{18}F]1** is higher than that of [^{18}F](2S, 4R)4-FGln at 60 min (2.06 ± 0.04) and 120 min (2.49 ± 0.08), so tumors delineated by **[^{18}F]1** PET imaging are easier. To the conclusion that **[^{18}F]1** and [^{18}F](2S, 4R)4-FGln are superior in the imaging of breast cancer, a more detailed comparison of biodistribution and PET imaging of nude mice bearing MCF-7 tumor is still required.

In summary, a new arginine analog **[^{18}F]1** was designed and prepared, which has simple synthesis conditions and a high yield. The labeling conditions of **[^{18}F]1** are mild and easy to handle, and their stability in vivo is high. **[^{18}F]1** showed the high cellular uptake of 7.3 ± 0.24% and 6.07 ± 0.3% uptake/100 mg protein after incubation in MCF-7 and MDA-MB-231 cells for 120 min, respectively. Inhibition experiments found that L-arginine was a more effective inhibitor than L-lysine and L-histidine, blocking 62% of the **[^{18}F]1** uptake. These properties allow the tracer to be a specific probe for cationic transporters in vivo. In vivo biodistribution studies have shown that **[^{18}F]1** provides high tumor uptake and high tumor to muscle ratio (approximately 5:1 at the 30 and 60 min time points). Small animal PET studies with **[^{18}F]1** demonstrated good tumor visualization of MCF-7 tumors up to 3 h p.i. These results support the conclusion that **[^{18}F]1** may be a promising candidate for the PET imaging of breast cancer. The specific role of arginine and its derivatives in the process of tumorigenesis and development is very complicated. Therefore, the use of **[^{18}F]1** is expected to reveal the function of arginine and nitric oxide, thereby revealing new intersections between metabolism and disease and finding new opportunities for therapeutic intervention.

3. Experimental section

Journal Pre-proof

3.1. General information

All reagents were commercial products used without further purification unless otherwise indicated. Deionized water used in our experiments was obtained from a Milli-Q water system. MCF-7 cells and MDA-MB-231 cells were obtained from the American, ATCC, Manassas, VA. Fetal bovine serums were purchased from Beijing YuanHeng ShenMa Biology Technology Research Institute. NMR spectra were recorded at 400 MHz at ambient temperature. Chemical shifts are reported in parts per million downfield from TMS (tetramethylsilane). Coupling constants in ^{1}H NMR are expressed in Hertz. High-resolution mass spectrometry (HRMS) data was obtained with an Agilent (Santa Clara, CA) G3250AA LC/MSD TOF system. Thin-layer chromatography (TLC) analyses were performed using Merck (Darmstadt, Germany) silica gel 60 F254 plates. Crude compounds were generally purified by flash column chromatography (FC) packed with Teledyne ISCO. Small animal PET imaging data were recorded on a microPET (Inveon, Siemens, Germany).

3.2. Synthesis

*tert-butyl (2S)-5-((E)-2,3-bis (tert-butoxycarbonyl)guanidino)-2- ((tert-butoxycarbonyl) amino)-4-hydroxypentanoate (**2**)* A solution of tert-butyl (2S)-5-amino-2-((tert- butoxycarbonyl) amino)-4-hydroxypentanoate (0.5 g, 1.64 mmol), N,N′-Di-Boc-1H-pyrazole -1-carboxamidine (0.28 g, 2 mmol) and N,N-Diisopropylethylamine (1 mL) at 50 ^{o}C in 30 mL acetonitrile for 3 h. The solvent was removed under vacuum, and purified by FC (ethyl acetate/hexane 30/70) to get little yellow oil **2** (0.77 g, 86.3%).^{1}H NMR (400 MHz, $CDCl_3$) δ 11.44 (s, 1H), 8.71 (s, 1H), 5.45 (s, 1H), 5.25 (s, 1H), 4.25 (s, 1H), 3.93 (s, 1H), 3.61 - 3.58 (m, 1H), 3.43-3.33 (m, 1H), 2.11 - 1.80 (m, 2H), 1.51 (s, 36H). ^{13}C NMR (101 MHz, $CDCl_3$) δ 171.60, 162.73, 157.54, 152.94, 83.49, 81.99, 79.53, 77.34, 77.02, 76.70, 69.06, 65.73, 51.96, 47.31, 37.48, 28.33, 28.18, 28.02, 27.98, 27.96. HRMS calcd for C25H47N4O9+, 547.3338 [M+H]$^+$; found, 547.3339.

*tert-butyl (2S)-5-((E)-2,3-bis(tert-butoxy carbonyl)guanidino)-2-((tert-butoxycarbonyl)amino)-4-((methylsulfonyl)oxy)pentanoate (**3**)* To a stirred solution of **2** (0.5 g, 0.91 mmol) in CH_2Cl_2 (25 mL) at 0 ^{o}C, Et_3N (0.3 mL, 2.7 mmol), Methanesulfonyl chloride (MsCl, 0.31 g, 2.7 mmol) and catalytic amount 4-dimethylaminopyridine (DMAP, 0.012 g, 0.1 mmol) were added sequentially. After maintaining at 0 ^{o}C for 15 min., the ice bath was removed, the reaction kept at room temperature for overnight. The solution was washed by H_2O, and dried by Na_2SO_4. The crude product was purified by FC (ethyl acetate /hexanes, 20/80) to provide a light yellow oil **3** (0.18 g, 32.6%). ^{1}H NMR (400 MHz, $CDCl_3$) δ 11.41 (s, 1H), 8.65 (s, 1H), 5.44 - 5.27 (m, 1H), 5.04 - 4.84 (m, 1H), 4.24 (m, 1H), 3.85 - 3.74 (m, 1H), 3.16 (s, 3H), 2.35 - 2.17 (m, 1H), 2.15 - 2.04 (m, 1H), 1.68 - 1.34 (m, 36H).^{13}C NMR (101 MHz, $CDCl_3$) δ 171.11, 170.64, 162.82, 156.57, 155.47, 152.88, 83.54, 82.27, 79.96, 77.92, 77.35, 77.04, 76.72, 60.36, 50.99, 44.35, 39.35, 38.29, 34.53, 28.29, 28.19, 28.01, 27.97, 27.93, 21.02, 14.18. HRMS calcd for C26H49N4O11S+, 625.3113[M+H]$^+$; found, 625.3114.

*(2S,4S)-5-(tert-butoxy)-4-((tert-butoxycarbonyl)amino)-5-oxo-2-(3-((tetrahydro-2H-pyran-2-yl)oxy)propyl)pentanoic acid (**7**)* A mixture of the ester **6** (1.5 g, 2.8 mmol) and 10% Pd/C (0.2 g) in absolute EtOH (20 mL) was stirred under H_2 for 3 h. This mixture was then filtered and the filtrate was concentrated under vacuum to give a white solid **7** (1.24 g, 100%). ^{1}HNMR (400 MHz, $CDCl_3$) δ: 5.09 (s, 1H), 4.58 (d, *J* = 4.0 Hz, 1H), 4.23 (d, *J* = 5.6 Hz, 1H), 4.0 (s, 1H), 3.86 (d, *J* = 6.0 Hz, 2H), 2.59-2.44 (m, 1H), 1.91 - 1.79 (m, 2H), 1.71 - 1.69 (m, 6H), 1.55-1.53 (m, 4H), 1.47 (s, 9H), 1.45 (s, 9H). ^{13}C NMR (100 MHz, $CDCl_3$) δ: 172.14, 159.40, 155.60, 129.16, 128.28, 114.36, 84.88, 83.24, 82.80, 81.85, 79.28, 55.31, 52.15, 50.95, 47.41, 35.58, 34.66, 28.31, 28.20. HRMS calcd for C22H40NO8+, 446.2748[M+H]$^+$; found, 446.2762.

*tert-butyl (2S,4S)-2-((tert-butoxycarbonyl) amino)-4-(hydroxymethyl)-7-((tetrahydro-2H-pyran-2 -yl)oxy)heptanoate (**8**)* Acid **7** (1 g, 2.24 mmol) was dissolved in 5 mL THF in a 50 mL round bottom flask and the solution was cooled to 0 ^{o}C. To this solution Et_3N (0.24 mL, 2.24 mmol) and ethyl chloroformate (0.21 mL, 2.79 mmol) were added dropwise. After stirring at 0 ^{o}C for 30 min, the reaction mixture was filtered off. To a mixture of $NaBH_4$ (0.17 g, 4.48 mmol) with 2 mL H_2O in a 100 mL round bottom flask cooled with an ice bath the above filtrate was added slowly. The mixture was stirred at room temperature for a further 1 h and was then acidified with 1 M HCl until the pH = 7 under cooling with ice bath. The organic phase was collected and water phase was extracted with ethyl acetate (20 mL × 3). The organic phases were combined, washed with Sat. $NaHCO_3$ (20 mL) and brine (20 mL), and dried with $MgSO_4$. The filtrate was evaporated in vacuo and the residue was purified by FC (ethyl acetate/hexane 30/70) to give an oil **8** (0.82 g, 85.2%). ^{1}HNMR (400 MHz, $CDCl_3$) δ: 5.21 (s, 1H), 4.58 (d, *J* = 4.8 Hz, 1H), 4.22 (s, 1H), 3.90 - 3.85 (m, 1H), 3.78 - 3.73 (m, 2H), 3.58 - 3.51 (m, 1H), 3.43 - 3.38 (m, 1H), 1.85 - 1.78 (m, 1H), 1.72 - 1.55 (m, 12H), 1.48 (s, 9H), 1.45 (s, 9H). ^{13}C NMR (100 MHz, $CDCl_3$) δ: 172.20, 155.54, 99.01, 67.77, 67.72, 64.87, 62.51, 62.47, 52.25, 37.43, 30.75, 28.32, 28.00, 27.96, 26.95, 25.45, 19.75, 19.73. HRMS calcd for C22H41NNaO7+, 454.2775[M+Na]$^+$; found,454.2740.

*tert-butyl (2S,4S)-4-(((E)-N,N'-bis(tert- butoxycarbonyl)-1H-pyrazole-1-carboximidamido) methyl)-2-((tert-butoxycarbonyl)amino) -7-((tetrahydro-2H-pyran-2-yl)oxy)heptanoate (**9**)* To a solution of N,N′-Di-Boc-1H-pyrazole-1-carboxamidine (0.58 g, 1.86 mmol), **8** (0.8 g, 1.86 mmol) and triphenylphosphine (0.49 g, 1.86 mmol) at 0 ^{o}C in anhydrous THF, diethyl azodicarboxylate (0.34 mL, 1.86 mmol) was added dropwise, after 10 min, the reaction was warmed at room temperature and stirred overnight. The solvent was removed under vacuum, and purified by FC (ethyl acetate/hexane 20/80) to get colorless oil **9** (1.2g, 89.1%). ^{1}HNMR (400 MHz, $CDCl_3$) δ: 7.95 (s, 1H), 7.68 (s, 1H), 6.37 - 6.36 (m, 1H), 6.07 (s, 1H), 4.48 (d, *J* = 1.2 Hz, 1H), 3.93 - 3.88 (m, 1H), 3.77 - 3.72 (m, 1H), 3.65 - 3.60 (m, 2H), 3.40 - 3.37 (m, 1H), 3.32 - 3.26 (m, 1H), 1.94 - 1.69 (m, 3H), 1.64 - 1.58 (m, 3H), 1.48 - 1.40 (m, 16H), 1.34 - 1.32 (m, 18H), 1.17 (s, 9H). ^{13}C NMR (100 MHz, $CDCl_3$) δ:172.40, 157.20, 156.14, 152.13, 143.16, 130.60, 109.07, 98.69, 98.53, 82.68, 82.56, 80.72, 18.69, 77.47, 77.15,, 76.38, 67.28, 67.17, 62.06, 60.20, 53.10, 52.15, 35.04, 34.90, 34.05, 30.06, 28.28, 28.19, 27.84, 27.80, 27.60, 26.48, 25.40, 19.47. HRMS calcd for C36H62N5O10+ 724.4491[M+H]$^+$; found, 724.4504.

*tert-butyl (2S,4S)-4-(((Z)-1,3-bis(tert- butoxycarbonyl)-2-(4-methoxybenzyl)guanidino)methyl)- 2-((tert-butoxycarbonyl)amino)-7- ((tetrahydro-2H-pyran-2-yl)oxy)heptanoate (**10**)* A solution of **9** (1 g, 1.38 mmol), 4-Methoxybenzylamine (0.28 g, 2 mmol) and *N,N*-Diisopropylethylamine (1 mL) at 50 ^{o}C in 30 mL acetonitrile for 3 h. The solvent was removed under vacuum, and purified by FC (ethyl acetate/hexane 30/70) to get little yellow oil **10** (0.71 g, 75.1%). ^{1}HNMR (400 MHz, $CDCl_3$) δ: 7.26 (d, *J* = 8.8Hz, 2H), 6.90 (d, *J* = 8.8Hz, 2H), 5.10 - 4.96 (m, 1H), 4.56 (s, 1H), 4.40 (s, 1H), 4.16 (s, 1H), 3.82 (s, 4H), 3.74 - 3.64 (m, 2H), 3.51 - 3.47 (m, 1H), 3.39 - 3.31 (m, 1H), 1.90 - 1.80 (m, 2H), 1.68 - 1.65 (m, 4H), 1.61 - 1.54 (m, 7H), 1.49 (s, 18H), 1.46 (s, 9H). ^{13}C NMR (100 MHz, $CDCl_3$) δ:172.27, 159.37, 129.22, 114.33, 98.73, 82.62, 81.67, 79.50, 79.24, 67.57, 67.50, 62.23, 60.39, 55.30,

Journal Pre-proof

52.36, 51.31, 47.37, 34.93, 30.70, 28.32, 28.22, 28.19, 27.99, 27.56, 26.06, 25.49, 21.95, 21.72, 21.05, 19.61, 14.20. HRMS calcd for C41H69N4O11+, 793.4957[M+H]$^+$; found, 793.4955.

*tert-butyl (2S,4S)-4-(((Z)-1,3-bis(tert-butoxy carbonyl)-2-(4-methoxybenzyl)guanidino)methyl) -2-((tert-butoxycarbonyl)amino)-7- hydroxyheptanoate **(11)*** A solution of **10** (1 g, 1.26 mmol) and Pyridinium *p*-toluenesulfonate (0.31 g, 1.26 mmol) at 50 ^{o}C in 30 mL ethanol for 2 h. Saturated $NaHCO_3$ (0.13 g, 1.26 mmol) was added, filtered. The solvent was removed under vacuum, and purified by FC (ethyl acetate/ hexane 40/60) to get white solid **11** (0.67 g, 84.2%). ^{1}HNMR (400 MHz, $CDCl_3$) δ: 9.38 (s, 1H), 7.26 (d, *J* = 8.8Hz, 2H), 6.90 (d, *J* = 8.8Hz, 2H), 5.05 - 5.01 (m, 1H), 4.40 - 4.30 (m, 2H), 4.20 (t, *J* = 8.0Hz, 1H), 3.87 - 3.82 (m, 1H), 3.79 (s, 1H), 3.61 - 3.49 (m, 3H), 2.81 (s, 1H), 1.79 (s, 1H), 1.65 - 1.60 (m, 6H), 1.54 - 1.52 (m, 18H), 1.48 (s, 9H), 1.46 (s, 9H). ^{13}C NMR (100 MHz, $CDCl_3$) δ: 172.15, 171.78, 159.39, 155.87, 153.65, 129.14, 128.21, 114.35, 114.22, 98.94, 98.88, 82.82, 81.92, 79.91, 79.25, 77.39, 77.07,76.76, 62.40, 62.37, 61.22, 60.34, 55.26, 55.22, 51.79, 50.68, 47.43, 44.75, 36.55, 33.31, 30.71, 28.47, 28.39, 28.29, 28.16, 28.13, 27.95, 25.77, 25.43, 20.99, 19.68. HRMS calcd for C36H61N4O10+, 709.4382[M+H]$^+$; found, 709.4381.

*tert-butyl (2S,4S)-4-(((Z)-1,3-bis(tert-butoxy carbonyl)-2-(4-methoxybenzyl)guanidino)methyl) -2-((tert-butoxycarbonyl)amino)-7- (tosyloxy)heptanoate **(12)*** To a stirred solution of **11** (0.8 g, 1.1 mmol) in CH_2Cl_2 (25 mL) at 0 ^{o}C, Et_3N (0.33 mL, 3.3 mmol), p-toluenesulfonyl chloride (TsCl, 0.418 g, 2.2 mmol) and catalytic amount 4-dimethylaminopyridine (DMAP, 0.11 mmol, 0.013 g) were added sequentially. After maintaining at 0 ^{o}C for 15 min., the ice bath was removed, the reaction kept at room temperature for overnight. The solution was washed by H_2O, and dried by Na_2SO_4. The crude product was purified by FC (ethyl acetate /hexanes, 30/70) to provide a light yellow oil **12** (0.7 g, 86.3%). $[\alpha]^{25}_D$ = - 41.3 (*c* = 1.0), MeOH. ^{1}HNMR (400 MHz, $CDCl_3$) δ: 9.46 (s, 1H), 7.76 (d, *J* = 8.8Hz, 2H), 7.32 (d, *J* = 8.8Hz, 2H), 7.23 (d, *J* = 8.8Hz, 2H), 6.89 (d, *J* = 8.8Hz, 2H), 5.04 (s, 1H), 4.36 (s, 2H), 4.09 (s, 1H), 4.00 - 3.97 (m, 2H), 1.47 - 1.46 (m, 18H), 1.43 (s, 9H), 1.40 (s, 9H). ^{13}C NMR (100 MHz, $CDCl_3$) δ: 171.97, 159.39, 155.59, 153.40, 144.59, 133.15, 129.81, 127.81, 114.36, 82.82, 81.87, 79.58, 79.28, 77.37, 77.25, 77.05, 76.74, 70.68, 60.36, 55.28, 55.12, 50.68, 47.35, 35.50, 34.65, 28.18, 28.15, 27.96, 26.76, 25.50. 21.59. HRMS calcd for C43H67N4O12S+, 863.4471[M+H]$^+$; found, 863.4475.

*tert-butyl (2S,4S)-4-(((Z)-1,3-bis(tert-butoxy carbonyl)-2-(4-methoxybenzyl)guanidino) methyl)- 2-((tert-butoxycarbonyl)amino)-7- fluoroheptanoate **(13)*** To a stirred solution of tris(dimethylamino) sulfonium difluorotrimethylsilicate (TASF, 1.38 g, 5.0 mmol) in CH_2Cl_2/THF (1.5 mL/1.5 mL) was added $Et_3N{\cdot}(HF)_3$ (0.25 mL) dropwise. The above solution was added to tosylate **12** (0.5 g, 0.58 mmol) in 5 mL THF, the reaction was stirred at 55 ^{o}C for overnight. The reaction mixture was diluted with ethyl acetate and washed with saturated $NaHCO_3$, water and brine subsequently. The ethyl acetate phase was collected, dried by $MgSO_4$, filtered, concentrated in vacuo. The left residue was purified by FC (ethyl acetate /hexanes, 20/80) to provide a light yellow oil **13** (0.23 g, 55.6%). $[\alpha]^{25}_D$ = - 30.2 (*c* = 1.0), MeOH. ^{1}HNMR (400 MHz, $CDCl_3$) δ: 7.27 (d, *J* = 8.8Hz, 2H), 6.91 (d, *J* = 8.8Hz, 2H), 5.01 (s, 1H), 4.48 (t, *J* = 6.0Hz, 1H), 4.39 (s, 1H), 4.19 - 4.14 (m, 1H), 3.82 (s, 1H), 3.80 - 3.75 (m, 1H), 3.66 - 3.61 (m, 1H), 1.86 (s, 1H), 1.82 - 1.54 (m, 6H), 1.49 (s, 18H), 1.45 (s, 9H), 1.42 (s, 9H). ^{13}C NMR (100 MHz, $CDCl_3$) δ: 172.14, 159.40, 155.60, 153.49, 129.16, 128.28, 114.36, 84.88, 83.24, 82.80, 81.85, 79.28, 55.31, 52.15, 50.95, 47.41, 35.58, 34.66, 28.31, 28.20, 28.17, 27.98. HRMS calcd for C36H60FN4O9+, 711.4339[M+H]$^+$; found, 711.4335.

*(2S, 4S)4-(3-fluoropropyl)Arginine **(2S,4S)4-FPArg**,* **1** A solution of **13** (0.1 g, 0.14 mmol) and trifluoroacetic acid (TFA, 5 mL) was stirred at room temperature for overnight. The solvent was removed under vacuum, diethyl ether was added, washed by diethyl ether, the sticky colorless oil in flask was collected, and purified by HPLC (30 mg, 93.7%). $[\alpha]^{25}_D$ = + 25.9 (*c* = 1.0), MeOH. ^{1}HNMR (400 MHz, D_2O) δ: 4.51 (t, *J* = 5.6Hz, 1H), 4.39 (t, *J* = 5.6Hz, 1H), 3.96 (t, *J* = 2.8Hz, 1H), 3.24 - 3.19 (m, 1H), 3.14 - 3.08 (m, 1H), 1.97 - 1.88 (m, 2H), 1.78 - 1.59 (m, 3H), 1.49 - 1.41 (m, 2H). ^{13}C NMR (100 MHz, D_2O) δ: 172.70, 157.02, 85.95, 84.37, 71.25, 51.37, 43.77, 33.37, 32.37, 26.14, 25.95, 21.07. ^{19}F NMR (376.5 MHz, CD_3OD): -220.34 (H-F decoupled). HRMS calcd for C9H20FN4O2+, 235.1565[M+H]$^+$; found, 235.1567.

3.3. Radiosynthesis

[^{18}F] Fluoride and ^{18}F-FDG was produced from department of Nuclear Medicine in Peking University Cancer Hospital & Institute with a HM-20 medical cyclotron (Sumitomo, Kyoto, Japan) as an [^{18}O] enriched aqueous solution of [^{18}F]fluoride. Solid-phase extraction (SPE) cartridges such as Sep-Pak QMA Light and Oasis HLB cartridges were purchased from Waters (Milford, MA). High performance liquid chromatography (HPLC) was performed on Agilent 1100 series system with different HPLC columns.

Typical radiosyntheses began with approximately 740 to 1480 MBq (20 to 40 mCi) of [^{18}F] fluoride. An activated SepPak Light QMA Carb was loaded with [^{18}F] fluoride and eluted with 1 mL of 18-crown-6/$KHCO_3$ (320 mg of 18-crown-6 in 18.6 mL of ACN/58 mg of $KHCO_3$ in 3.4 mL of water). The solution was blown with argon until dry and dried thrice azeotropically with 1 mL of acetonitrile at 100 ^{o}C under a flow of argon. The dried [^{18}F] fluoride was cooled in an ice bath and 5 mg of tosylate precursor **12** was dissolved in 1 mL of tert-amyl alcohol and acetonitrile (9/1), and added to the dried [^{18}F] fluoride. The mixture was heated for 15 min at 100 ^{o}C. The mixture was then cooled in an ice bath and added to 9 mL of water. The mixture was loaded onto an activated Oasis HLB 3 cm^3 cartridge, pushed through, and washed with 10 mL of water. The desired radiolabeled intermediate **[^{18}F]13** was eluted with 1 mL of ethanol. The radiochemical purity of the intermediate **[^{18}F]13** was assessed by coinjection of the nonradioactive cold **13**, onto an analytical column (Phenomenex Gemini-Nx C18 110A (250 × 4.6 mm × 5 μm) using a solution of 15/85 0.1% formic acid aqueous solution/acetonitrile as mobile phase with a flow rate of 1 mL/min and λ = 254 nm. **[^{18}F]13** had retention times of 16.5 min (Figure S2). The radiochemical purity was > 95%.

The ethanol solution was blown until dry. A mixture of TFA (0.495 mL) and anisole (5 μL) was added and heated for 5 min at 60 ^{o}C in a capped 10 mL vial. TFA was removed under argon while still warm. The reaction tube was then cooled in an ice bath. 1 mL of 10% ethanol physiological saline solution was slowly added into the mixture, vortexed and mixed, filtered by sterile membrane, yielded the desired radioactive (2S,4S)4-[^{18}F]FPArg, **[^{18}F]1**, (pH = 5 - 7). The radiochemical purity was > 95% (Figure 2b and S4b).

The radiochemical and stereochemical purities of **[^{18}F]1** were determined by two different HPLC systems. System 1. Column: Chirex 3126 (D)-penicillamine 250 × 4.6 mm, 4.6 μm. Mobile phase (isocratic): Methanol /1 mM $CuSO_4$ solution=5/95, 1 mL/min, column temperature at 30 ^{o}C. The retention times of **[^{18}F]1** are 11.6 min (Figure 2b). System 2. Methanol /1 mM $CuSO_4$ solution=10/90, 1 mL/min, column temperature at 30 ^{o}C.

Journal Pre-proof

The retention times of **[^{18}F]1** are 8.2 min (Figure S4b). The specific activity **[^{18}F]1** was > 11 GBq/μmol at the end of synthesis.

The labeling of **[^{18}F]25** follows the labeling method of **[^{18}F]1**. The radiochemical purity of the intermediate **[^{18}F]24** was assessed by coinjection of the nonradioactive standard **24**, onto an analytical column (Phenomenex Gemini-Nx C18 110A (250 × 4.6 mm × 5 μm) using a solution of 15/85 0.1% formic acid aqueous solution/acetonitrile as mobile phase with a flow rate of 1 mL/min and λ = 254 nm. **[^{18}F]24** had retention times of 16.2 min (Figure S5). The radiochemical purity was > 95%. The radiochemical and stereochemical purities of **[^{18}F]25** were determined by two different HPLC systems. System 1. Column: Chirex 3126 (D)-penicillamine 250 × 4.6 mm, 4.6 μm. Mobile phase (isocratic): Methanol /1 mM $CuSO_4$ solution=5/95, 1 mL/min, column temperature at 30 ^oC. The retention times of **[^{18}F]25** are 20.1 min (Figure S6). System 2. Methanol/1 mM $CuSO_4$ solution=10/90, 1 mL/min, column temperature at 30 ^oC. The retention times of **[^{18}F]25** are 14.6 min (Figure S6). The specific activity **[^{18}F]25** was > 11 GBq/μmol at the end of synthesis.

Partition Coefficient (Log P): The partition coefficients were measured by mixing **[^{18}F]1** (37 kBq) with 3 g each of 1-octanol and buffer (pH 7.4, 0.1 M phosphate) in a test tube. The test tube was then vortexed for 2 min and centrifuged for 10 min at room temperature. Two samples (2 g) from the 1-octanol and buffer layers were weighed and counted in a gamma counter. The partition coefficient was determined by calculating the ratio of counts per min/gram in octanol to that of the buffer. Samples of the 1-octanol layer were repartitioned until consistent partition coefficient values were obtained. The measurement was repeated three times

Stability in plasm: Fresh blood was collected into 1.5 mL heparin-coated EP tube from anesthetized C57BL/6 mice. Cells were removed by centrifugation for 10 min at 2000 g. The resulting supernatant was the plasma for test. Incubations were carried out at 37 °C in a water bath. Then the sample was taken and centrifuged for 5 min at 14 000 rpm, 10 μL of the supernatant layer was measured by radio-HPLC at 30, 60 and 120 min.

Stability in PBS: [^{18}F]1 (370 kBq) was added to 1 mL PBS (pH = 7.4, 0.1 M) solution. The solutions were incubated at room temperature for PBS. Then the sample was taken to radio-HPLC analysis to measure the stability in PBS at 30, 60 and 120 min.

3.4. Cell Uptake Assays and Inhibition Studies

MCF-7 cells were cultured in RPMI 1640 (SIGMA) supplemented with 10% fetal bovine serum (YHSM) and 1% penicillin/ streptomycin (Gibco). The cells were maintained in T-75 culture flasks under humidified incubator conditions (37 ^oC, 5% CO_2) and were routinely passaged at confluence. MDA-MB-231 cells were maintained in L-15 medium supplemented with 10% fetal calf serum and 1% penicillin / streptomycin (Gibco) at 37 ^oC in a humidified atmosphere of 5% CO_2 with the change of fluid 2-3 times per week. Tumor cells were plated (2.0×10^5 cells/well) 24 h in the media prior to ligand incubation. On the day of the experiment, the culture media was aspirated and the cells were washed three times with warm PBS (containing 0.90 mM of Ca^{2+} and 1.05 mM of Mg^{2+}). **[^{18}F]1**, **[^{18}F]FDG** or [^{18}F](2S, 4R)4-FGln (37 kBq/mL/well) were mixed in PBS, respectively(with Ca^{2+} and Mg^{2+}) solution and then added to each well. The cells were incubated at 37 °C for 5, 30, 60, and 120 min. At the end of the incubation period, the PBS solution containing the ligands was aspirated and the cells were washed three times with 1 mL of ice cold PBS (without Ca^{2+} and Mg^{2+}). After washing with ice-cold PBS, 350 μL of 1M NaOH was used to lyse the cells. The lysed cells were collected onto filter paper and counted together with samples of the incubation dose using a gamma counter. A total of 100 μL of the cell lysate was used to determine the protein concentration (Modified Lowry Protein Assay). The data was normalized as percentage uptake of initial dose (ID) relative to 100 μg of protein content (% ID/100 μg of protein).

To characterize the transport of **[^{18}F]1**, competitive inhibition studies were conducted using the MCF-7 cell line. Various inhibitors were then added to the cells in sodium PBS solution or sodium free PBS solution at a concentration of 10 mM. Selected inhibitors included synthetic amino acid transport inhibitors such as N-methyl-a-aminoisobutyric acid (MeAIB, 10 mM), a mixture of L-Ala/L-Ser/L-Cys (ASC, 3.3 mM of each amino acid), aminobicyclo(2,2,1)-heptane -2-carboxylic acid (BCH, 10 mM), L-arginine (Arg, 10 mM), L-lysine (Lys, 10 mM), L-histidine (His, 10 mM), and a mixture of L-Arg/L-Lys/L-His (RKH, 3.3 mM of each amino acid).[35] Natural amino acid arginine, lysine, histidine was also used as inhibitors. Two buffer conditions with and without sodium were used for the assays. In sodium free studies, the phosphate buffered saline solution contained 105 mM sodium chloride, 3.8 mM potassium chloride, 1.2 mM potassium bicarbonate, 25 mM sodium phosphate dibasic, 0.5 mM calcium chloride dehyrate, 1.2 mM magnesiumsulfate, and 5.6 mM D-glucose. In sodium free studies, PBS buffer was replaced with Na^+ free solution (143 mM choline chloride, 2.68 mM KCl and 1.47 mM KH_2PO_4).[53] The assays were performed as at pH 7.40 with each condition performed in 5 replicates. Briefly, cells were washed twice with 37 °C assay buffer (2 mL) and then incubated with different inhibitors (10 mM) for 30 min before starting the assay. The above cells are then incubated with **[^{18}F]1** (37 kBq/mL/well) in assay buffer for 30 min at 37 °C under the control or inhibitor conditions. The cells are then lysed and the protein concentration is calculated, which is consistent with cell uptake assays.

The IC_{50} assay was similar to inhibition studies. Different concentrations of arginine (0, 10^{-4}, 10^{-3}, 10^{-2}, 10^{-1}, 1, 2, 4, 5, 10, 20 mmol/L) or lysine (0, 2×10^{-4}, 2×10^{-3}, 2×10^{-2}, 2×10^{-1}, 2, 5, 10, 20, 40 mmol/L) were incubated with the above pretreated MCF-7 cells for 30 min, after which **[^{18}F]1** (74 kBq/mL/well) was added to the above cells and incubation was continued for 2 h. The cells are then lysed and the protein concentration is calculated, which is consistent with cell uptake assays. Competition experiments were analyzed using the GraphPad prism 7.00 nonlinear curve-fitting program to obtain half-maximal inhibitory concentrations (IC_{50}) values.

3.5. Biodistribution Studies.

Nude mice (female, weight, 12 - 16 g) bearing MCF-7 tumors (purchased from Cancer Hospital Chinese Academy of Medical Sciences, Beijing, China), MCF-7 cells ($\sim10^6$) in PBS (0.1 mL) were injected subcutaneously into the lower right flank of the nude mice. The tumors took 12-15 days to reach appropriate size (0.5 cm diameter). BALB/c mice (18-22 g) were purchase from Beijing Charles river Laboratories. All the animals were maintained according as the Chinese government guidelines for care and use of laboratory animals. Studies of the in vivo distribution of **[^{18}F]1** was performed in nude mice bearing MCF-7 tumors. Approximately 1.29 MBq **[^{18}F]1** or **[^{18}F]FDG** was administrated via tail vein injection in conscious animals. Groups of five animals were euthanized at 5, 30, 60, and 120 min p.i. All animals were not fasted prior to the study. The organs of interest were removed, weighed, and the radioactivity was counted with a gamma counter (Packard Cobra). The results were expressed as

the percent uptake of injected dose per gram of tissue (% ID/g) and presented as mean ± SD.

3.6. Small Animal PET/CT Imaging in nude Mice Bearing MCF-7 Tumors.

Dynamic small animal PET imaging studies were conducted with **[^{18}F]1** similar to that reported previously.[27] All scans were performed on a dedicated animal PET scanner (Inveon, Siemens, Germany). Nude mice with MCF-7 tumors were used for the imaging studies. A total of 8-11 MBq of activity was injected intravenously via the lateral tail vein. For blocking study, 0.5 mg or 2 mg of arginine was injected into nude mice 30 min before administration of **[^{18}F]1**, and PET images were collected for 45 - 65 min after administration. All animals were sedated with isoflurane anesthesia (2-3%, 1 L/min oxygen) and were then placed on a heating pad in order to maintain body temperature throughout the procedure. The animals were visually monitored for breathing and any other signs of distress throughout the entire imaging period. The data acquisition began after an intravenous injection of the tracer. All scans were conducted over a period of 180 min (dynamic, 5 min/frame). Regions of interest (ROIs) were drawn over tumor guided by CT images using Amira 3.1 image visualization and analysis software.

3.7. Statistical Analysis

Data were presented as mean ± standard deviation (SD). All statistical tests were conducted using the IBM SPSS Statistics Version 20.0 for Windows (SPSS, Inc., IBM Company). The independent samples nonparametric test was used to compare the difference of two quantitative groups. Pearson product-moment correlation coefficient (r) was used for correlation analysis between continuous variables.

Financial support

This research was supported by the National Natural Science Foundation of China (81701753) and Scientific Research Common Program of Beijing Municipal Commission of Education (KM201810025021 and KM201710025008).

Author contributions

Zehui Wu conceived and planned the experiments. Renbo Wu carried out the (radio)synthesis experiments. Song Liu, Yajing Liu, Yuli Sun, Xuebo Cheng, Yong Huang and Zequn Yang carried out the biological evaluation and PET imaging. Zehui Wu contributed to the interpretation of the results. Zehui Wu took the lead in writing the manuscript. All authors provided critical feedback and helped shape the research, analysis and manuscript. All authors have given approval to the final version of the manuscript.

Acknowledgements

We thank Professor Kung Hank F., Professor Zhu Lin and all members of their team. We also acknowledge Peking University Cancer Hospital PET Center, Core Facility Center of Capital Medical University and Captical Medical University Beijing Anzhen Hospital PET Center.

ABBREVIATIONS

ACN, Acetonitrile; 9-BBN, 9-Borabicyclo[3.3.1]nonane; CAT, cationic amino acid transporter; [^{11}C] MET, L-[^{11}C] methionine; [^{18}F] FET, O-(2-[^{18}F]fluoroethyl)-L-tyrosine; [^{123}I] IMT, [^{123}I] iodo-a-methyl tyrosine; [^{18}F] FDOPA, L-3,4-dihydroxy-6-[^{18}F]fluorophenyl alanine; [^{18}F] FMA, [^{18}F]-2-Amino-4-fluorobutanoic acid; S-[^{18}F] FAMP, (S)-2-amino-3-[^{18}F]fluoro-2-methylpropanoic acid S-[^{18}F] MeFAMP, [^{18}F] (2S,4R)4F-Glu, (2S,4R)-2-amino-4-(fluoro-^{18}F)pentanedioic acid; L-Ser, L-Serine; L-Cys, L-Cysteine; L-Ala, L-Alanine; LC-MS, Liquid Chromatography-Mass Spectrometrys; LiHMDS, Lithium bis(trimethylsilyl)amide; PPTS, Pyridinium p-toluenesulfonate; DHP, 3,4-Dihydro-2H-pyran; PBS, phosphate buffer saline; HPLC, high performance liquid chromatography; HRMS, High-resolution mass spectrometry; SUV, standardized uptake value; SD, standard deviation; TLC, thin-layer chromatography; TFA, trifluoroacetic acid.

Supplementary Material

Supplementary data (detailed procedure for the synthesis of (2R,4R)4-FPArg, **25**, analytical data, radiolabeling condition) associated with this article can be found in the online version, at. at doi:……

Reference

[1] McConathy J, Goodman Mark M. Non-natural amino acids for tumor imaging using positron emission tomography and single photon emission computed tomography. Cancer Metast. Rev. 27 (2008) 555-573.
[2] McConathy J, Yu W, Jarkas N, Seo W, Schuster DM, Goodman MM. Radiohalogenated nonnatural amino acids as PET and SPECT tumor imaging agents. Med. Res. Rev. 32 (2012) 868-905.
[3] Huang C, McConathy J. Radiolabeled amino acids for oncologic imaging. J. Nucl. Med. 54 (2013) 1007-1010.
[4] Zhu L, Ploessl K, Zhou R, Mankoff D, Kung HF. Metabolic Imaging of Glutamine in Cancer. J. Nucl. Med. 58 (2017) 533-537.
[5] Muller A, Chiotellis A, Keller C, Ametamey SM, Schibli R, Mu L, Kramer SD. Imaging tumour ATB0,+ transport activity by PET with the cationic amino acid O-2((2-[18F]fluoroethyl)methyl-amino)ethyltyrosine. Mol. Imaging Biol. 16 (2014) 412-420.
[6] Kanai Y, Hediger MA. The glutamate/neutral amino acid transporter family SLC1: molecular, physiological and pharmacological aspects. Pflugers Arch. 447 (2004) 469-479.
[7] Jungnickel KEJ, Parker JL, Newstead S. Structural basis for amino acid transport by the CAT family of SLC7 transporters. Nat. Commun. 9 (2018) 018-03066.
[8] Verrey F. System L: heteromeric exchangers of large, neutral amino acids involved in directional transport. Pflugers Arch. 445 (2003) 529-533.
[9] Closs EI, Boissel JP, Habermeier A, Rotmann A. Structure and function of cationic amino acid transporters (CATs). J. Membr. Biol. 213 (2006) 67-77.
[10] Nakanishi T, Tamai I. Solute carrier transporters as targets for drug delivery and pharmacological intervention for chemotherapy. J. Pharm. Sci. 100 (2011) 3731-3750.
[11] Ganapathy V, Thangaraju M, Prasad PD. Nutrient transporters in cancer: relevance to Warburg hypothesis and beyond. Pharmacol. Ther. 121 (2009) 29-40.
[12] Bouhlel A, Zhou D, Li A, Yuan L, Rich KM, McConathy J. Synthesis, Radiolabeling, and Biological Evaluation of (R)- and (S)-2-Amino-5-[(18)F]fluoro-2-methylpentanoic Acid ((R)-, (S)-[(18)F]FAMPe) as Potential Positron Emission Tomography Tracers for Brain Tumors. J. Med. Chem. 58 (2015) 3817-3829.
[13] Bouhlel A, Alyami W, Li A, Yuan L, Rich K, McConathy J. Effect of alpha-Methyl versus alpha-Hydrogen Substitution on Brain Availability and Tumor Imaging Properties of Heptanoic [F-18]Fluoroalkyl Amino Acids for Positron Emission Tomography (PET). J. Med. Chem. 59 (2016) 3515-3531.

Journal Pre-proof

Journal Pre-proof

[14] Chiotellis A, Muller Herde A, Rossler SL, Brekalo A, Gedeonova E, Mu L, Keller C, Schibli R, Kramer SD, Ametamey SM. Synthesis, Radiolabeling, and Biological Evaluation of 5-Hydroxy-2-[(18)F]fluoroalkyl-tryptophan Analogues as Potential PET Radiotracers for Tumor Imaging. J. Med. Chem. 59 (2016) 5324-5340.
[15] Leskinen-Kallio S, Nagren K, Lehikoinen P, Ruotsalainen U, Joensuu H. Uptake of 11C-methionine in breast cancer studied by PET. An association with the size of S-phase fraction. Br. J. Cancer. 64 (1991) 1121-1124.
[16] Singhal T, Narayanan TK, Jain V, Mukherjee J, Mantil J. 11C-L-methionine positron emission tomography in the clinical management of cerebral gliomas. Molecular Imaging and Biology. 10 (2008) 1-18.
[17] Hutterer M, Nowosielski M, Putzer D, Waitz D, Tinkhauser G, Kostron H, Muigg A, Virgolini IJ, Staffen W, Trinka E, Gotwald T, Jacobs AH, Stockhammer G. O-(2-18F-fluoroethyl)-L-tyrosine PET predicts failure of antiangiogenic treatment in patients with recurrent high-grade glioma. J. Nucl. Med. 52 (2011) 856-864.
[18] Pauleit D, Stoffels G, Bachofner A, Floeth FW, Sabel M, Herzog H, Tellmann L, Jansen P, Reifenberger G, Hamacher K, Coenen HH, Langen K-J. Comparison of 18F-FET and 18F-FDG PET in brain tumors. Nucl. Med. Biol. 36 (2009) 779-787.
[19] Pöpperl G, Kreth FW, Mehrkens JH, Herms J, Seelos K, Koch W, Gildehaus FJ, Kretzschmar HA, Tonn JC, Tatsch K. FET PET for the evaluation of untreated gliomas: correlation of FET uptake and uptake kinetics with tumour grading. Eur. J. Nucl. Med. Mol. I. 34 (2007) 1933-1942.
[20] Minn H, Kauhanen S, Seppanen M, Nuutila P. 18F-FDOPA: a multiple-target molecule. J. Nucl. Med. 50 (2009) 1915-1918.
[21] Koerts J, Leenders KL, Koning M, Portman AT, van Beilen M. Striatal dopaminergic activity (FDOPA-PET) associated with cognitive items of a depression scale (MADRS) in Parkinson's disease. Eur. J. Neurosci. 25 (2007) 3132-3136.
[22] Pauleit D, Floeth F, Tellmann L, Hamacher K, Hautzel H, Muller HW, Coenen HH, Langen KJ. Comparison of O-(2-18F-fluoroethyl)-L-tyrosine PET and 3-123I-iodo-alpha-methyl-L-tyrosine SPECT in brain tumors. J. Nucl. Med. 45 (2004) 374-381.
[23] Wang L, Zha Z, Qu W, Qiao H, Lieberman BP, Plössl K, Kung HF. Synthesis and evaluation of 18F labeled alanine derivatives as potential tumor imaging agents. Nucl. Med. Biol. 39 (2012) 933-943.
[24] Qu W, Oya S, Lieberman BP, Ploessl K, Wang L, Wise DR, Divgi CR, Chodosh LA, Thompson CB, Kung HF. Preparation and characterization of L-[5-11C]-glutamine for metabolic imaging of tumors. J. Nucl. Med. 53 (2012) 98-105.
[25] Qu W, Zha Z, Ploessl K, Lieberman BP, Zhu L, Wise DR, Thompson CB, Kung HF. Synthesis of optically pure 4-fluoro-glutamines as potential metabolic imaging agents for tumors. J. Am. Chem. Soc. 133 (2011) 1122-1133.
[26] Ploessl K, Wang L, Lieberman BP, Qu W, Kung HF. Comparative evaluation of 18F-labeled glutamic acid and glutamine as tumor metabolic imaging agents. J. Nucl. Med. 53 (2012) 1616-24.
[27] Wu Z, Zha Z, Li G, Lieberman BP, Choi SR, Ploessl K, Kung HF. [(18)F](2S,4S)-4-(3-Fluoropropyl)glutamine as a tumor imaging agent. Mol. Pharm. 11 (2014) 3852-3866.
[28] Turkbey B, Mena E, Shih J, Pinto PA, Merino MJ, Lindenberg ML, Bernardo M, McKinney YL, Adler S, Owenius R, Choyke PL, Kurdziel KA. Localized Prostate Cancer Detection with (18)F FACBC PET/CT: Comparison with MR Imaging and Histopathologic Analysis. Radiology. 270 (2014) 849-856.
[29] McConathy J, Martarello L, Malveaux EJ, Camp VM, Simpson NE, Simpson CP, Bowers GD, Olson JJ, Goodman MM. Radiolabeled amino acids for tumor imaging with PET: radiosynthesis and biological evaluation of 2-amino-3-[18F]fluoro-2-methylpropanoic acid and 3-[18F]fluoro-2-methyl-2-(methylamino)propanoic acid. J Med. Chem. 45 (2002) 2240-2249.
[30] Smolarz K, Krause BJ, Graner FP, Wagner FM, Hultsch C, Bacher-Stier C, Sparks RB, Ramsay S, Fels LM, Dinkelborg LM, Schwaiger M. (S)-4-(3-18F-fluoropropyl)-L-glutamic acid: an 18F-labeled tumor-specific probe for PET/CT imaging--dosimetry. J. Nucl. Med. 54 (2013) 861-866.
[31] Dunet V, Rossier C, Buck A, Stupp R, Prior JO. Performance of 18F-fluoro-ethyl-tyrosine (18F-FET) PET for the differential diagnosis of primary brain tumor: a systematic review and Metaanalysis. J. Nucl. Med. 53 (2012) 207-214.
[32] Fueger BJ, Czernin J, Cloughesy T, Silverman DH, Geist CL, Walter MA, Schiepers C, Nghiemphu P, Lai A, Phelps ME, Chen W. Correlation of 6-18F-fluoro-L-dopa PET uptake with proliferation and tumor grade in newly diagnosed and recurrent gliomas. J. Nucl. Med. 51 (2010) 1532-1538.
[33] Liu F, Xu X, Zhu H, Zhang Y, Yang J, Zhang L, Li N, Zhu L, Kung HF, Yang Z. PET Imaging of (18)F-(2 S,4 R)4-Fluoroglutamine Accumulation in Breast Cancer: From Xenografts to Patients. Mol. Pharm. 15 (2018) 3448-3455.
[34] Baek S, Mueller A, Lim YS, Lee HC, Lee YJ, Gong G, Kim JS, Ryu JS, Oh SJ, Lee SJ, Bacher-Stier C, Fels L, Koglin N, Schatz CA, Dinkelborg LM, Moon DH. (4S)-4-(3-18F-fluoropropyl)-L-glutamate for imaging of xC transporter activity in hepatocellular carcinoma using PET: preclinical and exploratory clinical studies. J. Nucl. Med. 54 (2013) 117-123.
[35] McConathy J, Zhou D, Shockley SE, Jones LA, Griffin EA, Lee H, Adams SJ, Mach RH. Click synthesis and biologic evaluation of (R)- and (S)-2-amino-3-[1-(2-[18F]fluoroethyl)-1H-[1,2,3]triazol-4-yl]propanoic acid for brain tumor imaging with positron emission tomography. Mol. Imaging. 9 (2010) 329-342.
[36] Prudner BC, Sun F, Kremer JC, Xu J, Huang C, Sai KKS, Morgan Z, Leeds H, McConathy J, Van Tine BA. Amino Acid Uptake Measured by [(18)F]AFETP Increases in Response to Arginine Starvation in ASS1-Deficient Sarcomas. Theranostics. 8 (2018) 2107-2116.
[37] Chantranupong L, Scaria SM, Saxton RA, Gygi MP, Shen K, Wyant GA, Wang T, Harper JW, Gygi SP, Sabatini DM. The CASTOR Proteins Are Arginine Sensors for the mTORC1 Pathway. Cell. 165 (2016) 153-164.
[38] Abdelmagid SA, Rickard JA, McDonald WJ, Thomas LN, Too CK. CAT-1-mediated arginine uptake and regulation of nitric oxide synthases for the survival of human breast cancer cell lines. J. Cell. Biochem. 112 (2011) 1084-1092.
[39] Saxton RA, Chantranupong L, Knockenhauer KE, Schwartz TU, Sabatini DM. Mechanism of arginine sensing by CASTOR1 upstream of mTORC1. Nature. 536 (2016) 229-233.
[40] Morris SM, Jr. Arginine Metabolism Revisited. J. Nutr. 146 (2016) 9.
[41] Vissers YL, Dejong CH, Luiking YC, Fearon KC, von Meyenfeldt MF, Deutz NE. Plasma arginine concentrations are reduced in cancer patients: evidence for arginine deficiency? Am J Clin Nutr. 81 (2005) 1142-1146.
[42] Ensor CM, Holtsberg FW, Bomalaski JS, Clark MA. Pegylated arginine deiminase (ADI-SS PEG20,000 mw) inhibits human melanomas and hepatocellular carcinomas in vitro and in vivo. Cancer Res. 62 (2002) 5443-5450.
[43] Feichtinger K, Sings HL, Baker TJ, Matthews K, Goodman M. Triurethane-Protected Guanidines and Triflyldiurethane-Protected Guanidines: New Reagents for Guanidinylation Reactions. J. Org. Chem. 63 (1998) 8432-8439.
[44] Kim DW, Jeong HJ, Lim ST, Sohn MH, Katzenellenbogen JA, Chi DY. Facile nucleophilic fluorination reactions using tert-alcohols as a reaction medium: significantly enhanced reactivity of alkali metal fluorides and improved selectivity. J. Org. Chem. 73 (2008) 957-962.
[45] Kim DW, Ahn D-S, Oh Y-H, Lee S, Kil HS, Oh SJ, Lee SJ, Kim JS, Ryu JS, Moon DH, Chi DY. A New Class of SN2 Reactions Catalyzed by Protic Solvents: Facile Fluorination for Isotopic Labeling of Diagnostic Molecules. J. Am. Chem. Soc. 128 (2006) 16394-16397.
[46] Abdelmagid SA, Rickard JA, McDonald WJ, Thomas LN, Too CKL. CAT-1-mediated arginine uptake and regulation of nitric oxide synthases for the survival of human breast cancer cell lines. J. Cell. Biochem. 112 (2011) 1084-1092.

[47] Closs EI, Simon A, Vekony N, Rotmann A. Plasma membrane transporters for arginine. J. Nutr. 134 (2004) 2752-2759.
[48] Fotiadis D, Kanai Y, Palacín M. The SLC3 and SLC7 families of amino acid transporters. Mol. Aspects Med. 34 (2013) 139-158.
[49] Closs EI, Boissel JP, Habermeier A, Rotmann A. Structure and Function of Cationic Amino Acid Transporters (CATs). J. Membrane Biol. 213 (2006) 67-77.
[50] Windmueller HG, Spaeth AE. Metabolism of absorbed aspartate, asparagine, and arginine by rat small intestine in vivo. Arch. Biochem. Biophys. 175 (1976) 670-676.
[51] Inoue Y, Bode BP, Beck DJ, Li AP, Bland KI, Souba WW. Arginine transport in human liver. Characterization and effects of nitric oxide synthase inhibitors. Ann. surg. 218 (1993) 350-363.
[52] Chiotellis A, Muller A, Weyermann K, Leutwiler DS, Schibli R, Ametamey SM, Kramer SD, Mu L. Synthesis and preliminary biological evaluation of O-2((2-[(18)F]fluoroethyl)methylamino)ethyltyrosine ([(18)F]FEMAET) as a potential cationic amino acid PET tracer for tumor imaging. Amino Acids. 46 (2014) 1947-1959.
[53] Lieberman BP, Ploessl K, Wang L, Qu W, Zha Z, Wise DR, Chodosh LA, Belka G, Thompson CB, Kung HF. PET imaging of glutaminolysis in tumors by 18F-(2S,4R)4-fluoroglutamine. J. Nucl. Med. 52 (2011) 1947-1955.

Journal Pre-proof

Journal Pre-proof

Highlights

Arginine derivative **[^{18}F]1** and **[^{18}F]25** were prepared;
[^{18}F]1 may be a high-affinity CAT-1 transporter substrate;
[^{18}F]1 showed high tumor uptake and high tumor to muscle ratios;
[^{18}F]1 is a promising tracer for clinical breast cancer imaging.

Journal Pre-proof